

Received December 1, 2018, accepted January 9, 2019, date of publication January 24, 2019, date of current version February 14, 2019.

Digital Object Identifier 10.1109/ACCESS.2019.2894788

A Novel Efficient WLP-Based BOR FDTD Method With Explicit Treating Ideology

DA-WEI ZHU^{1,2}, HAI-LIN CHEN¹, JIE YANG², YUN YI¹, AND BIN CHEN¹, (Member, IEEE)

¹National Key Laboratory on Electromagnetic Environmental Effects and Electro-Optical Engineering, PLA Army Engineering University, Nanjing 210007, China

²Nanjing Institute of Technology, Nanjing 211167, China

Corresponding author: Hai-Lin Chen (hylinchen@126.com)

This work was supported in part by the National Science Foundations of China under Grant 51477182 and Grant 61701221.

ABSTRACT In this paper, we proposed a novel efficient weighted Laguerre polynomial (WLP)-based finite-difference time-domain (FDTD) method with explicit treating ideology, which is extremely useful for problems with very fine structures in the body of revolution (BOR) system. By combining the explicit treating ideology and WLP technology, the limitation of time step Δt is effectively eliminated, which results in greatly improved performance. The performing idea of the proposed method can be roughly divided into two parts. First, the conventional WLP-based BOR FDTD method is flexibly transformed into a new one with certain direction explicit calculation by matrix transformation. Second, the initial value calculation and iteration calculation which are based on the different perturbation term are introduced to improve the convergence speed, the efficiency and accuracy of the proposed method. Meanwhile, the proofing results show that the convergence condition of the proposed method is relaxed. The stability analysis shows that the stability condition is determined by the smaller one of the spatial increments $\Delta\rho$ and Δz . Finally, two scattering numerical examples are given to demonstrate the computational accuracy and efficiency of the proposed method.

INDEX TERMS Body of revolution, explicit treating ideology, finite-difference time-domain, perturbation term, weighted Laguerre polynomial.

I. INTRODUCTION

Finite-difference time-domain (FDTD) method has been recognized as a powerful method for computational electromagnetics. It is a full-wave algorithm and does not need matrix inversion, which makes it have the advantages of saving operation and storage space, being suitable for parallel computing and generalization of computing program. In practical application, there are a large number of axisymmetric structures in electromagnetic field numerical calculation, for example, coaxial line, circular waveguide, antenna, missile, and aircraft fuselage [1]–[5]. In order to simulate these problems accurately, three-dimensional (3-D) cylindrical coordinate system can be used. However, due to the large amount of calculation caused by 3-D space, many electrically large metallic structures cannot be processed. Based on some symmetry of the field distribution around the axisymmetric structure, the body of revolution finite-difference time-domain (BOR-FDTD) method can be used to transform original 3-D problems (ρ, φ, z) into two dimensional (2-D) spaces (ρ, z) [6]. Compared with the 3-D FDTD method in cylindrical coordinate system, the BOR-FDTD method can greatly reduce the CPU time and memory space.

In recent years, the BOR-FDTD method has been widely used to model the electromagnetic wave problems. However, its time step should be limited by the Courant-Friedrich-Lecy stability condition [7]. To remove the stability limit on the time step of the BOR-FDTD method, the researchers did a large amount of studies which can be roughly divided into two directions. One was applying the alternating-direction implicit (ADI) FDTD scheme [8]–[10] to the BOR-FDTD method [11]. The other was applying the unconditionally stable weighted Laguerre polynomial (WLP) FDTD scheme [12] to the BOR-FDTD method [13]. Both of them can eliminate the CFL stability condition of original BOR-FDTD method and make the simulation more effective. However, the ADI scheme would lead a large numerical dispersion error when the time step is large [14], [15], and the unconditionally WLP one would lead to a large amount of memory requirement.

In order to overcome these problems of ADI and WLP schemes, researchers have done a lot of follow-up research. Among them, the study on ADI scheme includes local one-dimensional BOR-FDTD method [16], the weakly conditionally stable (WCS) BOR-FDTD method [17], [18]

and so on. These schemes for BOR have successfully achieved better efficiency. However, the LOD-BOR-FDTD method shows slight improvement in efficiency compared with the ADI one at the same accuracy. Although the WCS-BOR-FDTD method shows good accuracy and computational efficiency, it used four tri-diagonal equations and six explicit equations in the whole time step iteration process which still led to a certain degree of dispersion error at the high frequency range.

Recently, a new WLP scheme for BOR-FDTD method was developed by Wang *et al.* [19]. It used a new perturbation term and applied the Gauss-Seidel technology. As discussed in [19], the new perturbation term showed better convergence, especially at the high frequency range. Meanwhile, this new scheme showed higher accuracy and efficiency than other schemes [19]. And the problem of memory consumption has also been well addressed.

For some BOR structures, there are only fine structures in one direction, such as radial or axial direction. In this paper, to efficiently solve the electromagnetic problem of BOR structures with fine structure in one direction, we propose a novel efficient WLP based BOR-FDTD method with explicit treating ideology. Firstly, a new coefficient matrix is proposed by the ideology of the WCS-BOR-FDTD method to form the new matrix equations with certain direction explicit. And then, different perturbation terms are added to the new matrix equation to form the initial value calculation and iteration calculation schemes, so as to reduce the splitting error and improve the convergence speed. Secondly, the field components on z -axis are amended with special treatment. Finally, to verify the proposed method, two scattering numerical examples are given. Numerical results show that the proposed method is superior to the existing one-step WCS BOR-FDTD method and WLP based-BOR-FDTD method at efficiency, accuracy and memory consumption.

The remaining sections of the paper are organized as follows. Section II describes the principle of realization for the proposed explicit calculation scheme at ρ -direction. Section III introduces the explicit calculation scheme at z -direction. Section IV shows the convergence analysis and numerical stability proof. Finally, scattering numerical examples are simulated and analyzed.

II. PRINCIPLE OF REALIZATION FOR THE PROPOSED METHOD AT ρ DIRECTION

An isotropic lossless region with permittivity ϵ and permeability μ is considered. FIGURE 1 shows the Yee distribution of the electromagnetic field components of the proposed method.

A. REALIZING A NEW COEFFICIENT MATRIX

In [13], the equations of the conventional WLP based BOR-FDTD method can be rewritten as the following matrix form

$$(I - A - B)W^q = V^{q-1} \quad (1)$$

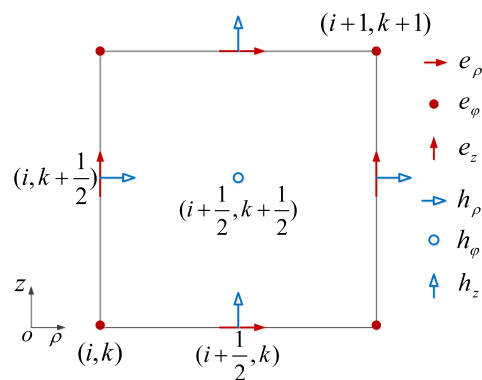


FIGURE 1. The distribution of the electromagnetic field components in the BOR-Yee grid.

Note that,

$$W^q = [W_E^q \ W_H^q]^T, \quad V^{q-1} = [V_E^{q-1} \ V_H^{q-1}]^T,$$

$$W_E^q = [e_\rho^q \ e_\phi^q \ e_z^q]^T, \quad W_H^q = [h_\rho^q \ h_\phi^q \ h_z^q]^T,$$

$$V_E^{q-1} = \begin{bmatrix} -2 \sum_{k=0}^{q-1} e_\rho^k & -2 \sum_{k=0}^{q-1} e_\phi^k & -2 \sum_{k=0}^{q-1} e_z^k \end{bmatrix}^T,$$

$$V_H^{q-1} = \begin{bmatrix} -2 \sum_{k=0}^{q-1} h_\rho^k & -2 \sum_{k=0}^{q-1} h_\phi^k & -2 \sum_{k=0}^{q-1} h_z^k \end{bmatrix}^T.$$

where I is a 6×6 identity matrix, q is the order of the WLP.

Referring to the ideology of the WCS BOR-FDTD method [17], [18], we can obtain the new coefficient matrix form.

$$A = \begin{bmatrix} 0 & \chi_{AH} \\ \chi_{AE} & 0 \end{bmatrix}, \quad B = \begin{bmatrix} 0 & \chi_{BH} \\ \chi_{BE} & 0 \end{bmatrix},$$

$$\chi_{AH} = \begin{bmatrix} 0 & 0 & a(\pm m/\rho) \\ 0 & 0 & -a(\partial/\partial\rho) \\ -a(\pm m/\rho) & 0 & 0 \end{bmatrix},$$

$$\chi_{AE} = \begin{bmatrix} 0 & 0 & -b(\mp m/\rho) \\ 0 & 0 & b(\partial/\partial\rho) \\ b(\mp m/\rho) & 0 & 0 \end{bmatrix},$$

$$\chi_{BH} = \begin{bmatrix} 0 & -a(\partial/\partial z) & 0 \\ a(\partial/\partial z) & 0 & 0 \\ 0 & a((\partial/\partial\rho) + (1/\rho)) & 0 \end{bmatrix},$$

$$\chi_{BE} = \begin{bmatrix} 0 & b(\partial/\partial z) & 0 \\ -b(\partial/\partial z) & 0 & 0 \\ 0 & -b((\partial/\partial\rho) + (1/\rho)) & 0 \end{bmatrix},$$

$$a = 2/s\epsilon, \quad b = 2/s\mu.$$

where $s > 0$ is the time-scale factor, m is the mode number, ∂/∂_i are the first order central difference operators along ρ and z , respectively.

Obviously, equation (1) needs to be decomposed that is similar with the existing WCS BOR-FDTD method or efficient WLP based-BOR-FDTD method to form the equation for ρ -direction explicit calculation.

B. REALIZING THE INITIAL VALUE CALCULATION

In [20] and [21], another efficient WLP scheme applied in rectangular coordinate system was introduced. Theoretical derivations and numerical examples showed that the perturbation term of this efficient WLP scheme can reduce the splitting error and get better efficiency and convergence speed than the conventional one. Applying this perturbation technique to BOR system and introducing $\mathbf{AB}(\mathbf{W}^q - \mathbf{V}^{q-1})$ term into equation (1), one can obtain

$$(\mathbf{I} - \mathbf{A})(\mathbf{I} - \mathbf{B})\mathbf{W}^q = (\mathbf{I} + \mathbf{AB})\mathbf{V}^{q-1} \tag{2}$$

By introducing a nonphysical intermediate value vector $\mathbf{W}^{*q} = [\mathbf{W}_E^{*q} \ \mathbf{W}_H^{*q}]^T = [e_\rho^{*q} \ e_\varphi^{*q} \ e_z^{*q} \ h_\rho^{*q} \ h_\varphi^{*q} \ h_z^{*q}]^T$, equation (2) can be divided into two steps.

$$(\mathbf{I} - \mathbf{A})\mathbf{W}^{*q} = (\mathbf{I} + \mathbf{B})\mathbf{V}^{q-1} \tag{3a}$$

$$(\mathbf{I} - \mathbf{B})\mathbf{W}^q = \mathbf{W}^{*q} - \mathbf{B}\mathbf{V}^{q-1} \tag{3b}$$

Equations (3a) and (3b) are the basic equations for the initial value calculation of the proposed method.

Substituting matrixes \mathbf{A} and \mathbf{B} into equations (3a) and (3b), one can obtain

$$\mathbf{W}_E^{*q} - \chi_{AH} \mathbf{W}_H^{*q} = \mathbf{V}_E^{q-1} + \chi_{BH} \mathbf{V}_H^{q-1} \tag{4a}$$

$$\mathbf{W}_H^{*q} - \chi_{AE} \mathbf{W}_E^{*q} = \mathbf{V}_H^{q-1} + \chi_{BE} \mathbf{V}_E^{q-1} \tag{4b}$$

$$\mathbf{W}_E^q - \chi_{BH} \mathbf{W}_H^q = \mathbf{W}_E^{*q} - \chi_{BH} \mathbf{V}_H^{q-1} \tag{4c}$$

$$\mathbf{W}_H^q - \chi_{BE} \mathbf{W}_E^q = \mathbf{W}_H^{*q} - \chi_{BE} \mathbf{V}_E^{q-1} \tag{4d}$$

Continuing to merge and tidy up equations (4a) ~ (4d), one can obtain

$$(\mathbf{I} - \chi_{AH} \chi_{AE})\mathbf{W}_E^{*q} = (\mathbf{I} + \chi_{AH} \chi_{BE})\mathbf{V}_E^{q-1} + (\chi_{AH} + \chi_{BH})\mathbf{V}_H^{q-1} \tag{5a}$$

$$(\mathbf{I} - \chi_{BH} \chi_{BE})\mathbf{W}_H^{*q} = (\mathbf{I} + \chi_{BH} \chi_{AE})\mathbf{W}_E^{*q} \tag{5b}$$

$$\mathbf{W}_H^q = \chi_{BE} \mathbf{W}_E^q + \chi_{AE} \mathbf{W}_E^{*q} + \mathbf{V}_H^{q-1} \tag{5c}$$

Substituting matrixes χ_{AH} , χ_{AE} , χ_{BH} , χ_{BE} into (5a) ~ (5c), one can obtain the FDTD expanding forms for the initial value calculation of the proposed method.

$$\begin{aligned} & (1 + ab(m^2/\rho^2)) e_\rho^{*q} \\ &= -2 \sum_{k=0}^{q-1} e_\rho^k \pm 2ab(m/\rho)(\partial/\partial\rho + 1/\rho) \sum_{k=0}^{q-1} e_\varphi^k \\ & \quad + 2a(\partial/\partial z) \sum_{k=0}^{q-1} h_\varphi^k \mp 2a(m/\rho) \sum_{k=0}^{q-1} h_z^k \end{aligned} \tag{6a}$$

$$\begin{aligned} e_\varphi^{*q} &= -2 \sum_{k=0}^{q-1} e_\varphi^k - 2ab(\partial/\partial\rho)(\partial/\partial\rho + 1/\rho) \sum_{k=0}^{q-1} e_\rho^k \\ & \quad \pm ab(\partial/\partial\rho)(m/\rho) e_\rho^{*q} - 2a(\partial/\partial z) \sum_{k=0}^{q-1} h_\rho^k \\ & \quad + 2a(\partial/\partial\rho) \sum_{k=0}^{q-1} h_z^k \end{aligned} \tag{6b}$$

$$\begin{aligned} & (1 + ab(m^2/\rho^2)) e_z^{*q} \\ &= -2 \sum_{k=0}^{q-1} e_z^k \pm 2ab(m/\rho)(\partial/\partial z) \sum_{k=0}^{q-1} e_\varphi^k \\ & \quad \pm 2ab(m/\rho) \sum_{k=0}^{q-1} h_\rho^k - 2ab(\partial/\partial\rho + 1/\rho) \sum_{k=0}^{q-1} h_\varphi^k \end{aligned} \tag{6c}$$

$$\begin{aligned} & (1 - ab(\partial/\partial z)) e_\rho^q \\ &= e_\rho^{*q} - ab(\partial/\partial z)(\partial/\partial\rho) e_z^{*q} \end{aligned} \tag{6d}$$

$$\begin{aligned} & (1 - ab(\partial/\partial z)) e_\varphi^q \\ &= e_\varphi^{*q} \pm ab(\partial/\partial z)(m/\rho) e_z^{*q} \end{aligned} \tag{6e}$$

$$\begin{aligned} e_z^q &= -ab(\partial/\partial\rho + 1/\rho)(\partial/\partial z) e_\rho^q \\ & \quad + (1 + ab(\partial/\partial\rho + 1/\rho)(\partial/\partial\rho)) e_z^{*q} \end{aligned} \tag{6f}$$

$$h_\rho^q = b(\partial/\partial z) e_\varphi^q \pm b(m/\rho) e_z^{*q} - 2 \sum_{k=0}^{q-1} h_\rho^k \tag{6g}$$

$$h_\varphi^q = -b(\partial/\partial z) e_\rho^q + b(\partial/\partial\rho) e_z^{*q} - 2 \sum_{k=0}^{q-1} h_\varphi^k \tag{6h}$$

$$h_z^q = -b(\partial/\partial\rho + 1/\rho) e_\varphi^q \mp b(m/\rho) e_\rho^{*q} - 2 \sum_{k=0}^{q-1} h_z^k \tag{6i}$$

Obviously, equations (6) are calculated based on the explicitly at the ρ -direction. Meanwhile, observing equations (6) and comparing with the initial value calculation of existing efficient WLP based-BOR-FDTD method [19], it is found that the former has only two tri-diagonal equations and the latter has four tri-diagonal equations. Thus, the efficiency of the initial value calculation in the proposed method is obviously better than that of the existing one.

C. REALIZING THE ITERATIVE CALCULATION

The introduction way of the perturbation term $\mathbf{AB}(\mathbf{W}_{p+1}^q - \mathbf{W}_p^q)$ in [19] is adopted into the equation (1), directly. One can obtain.

$$(\mathbf{I} - \mathbf{A})(\mathbf{I} - \mathbf{B})\mathbf{W}_{p+1}^q = \mathbf{AB}\mathbf{W}_p^q + \mathbf{V}^{q-1} \tag{7}$$

Note that, \mathbf{W}_p^q is the computational result of the initial value calculation, thus, the equation (7) is the computational result of the $(p + 1)th$ iteration. And the coefficient matrixes which include \mathbf{A} , \mathbf{B} , χ_{AH} , χ_{AE} , χ_{BH} and χ_{BE} are same with the initial value calculation of the proposed method.

Introducing the same nonphysical intermediate value vector \mathbf{W}^{*q} as the initial value calculation into equation (7), one can obtain the basic equations of the iteration calculation.

$$(\mathbf{I} - \mathbf{A})\mathbf{W}^{*q} = \mathbf{B}\mathbf{W}_p^q + \mathbf{V}^{q-1} \tag{8a}$$

$$(\mathbf{I} - \mathbf{B})\mathbf{W}_{p+1}^q = \mathbf{W}^{*q} - \mathbf{B}\mathbf{W}_p^q \tag{8b}$$

Substituting the coefficient matrixes \mathbf{A} and \mathbf{B} into (8a) and (8b), one can obtain.

$$\mathbf{W}_E^{*q} - \chi_{AH} \mathbf{W}_H^{*q} = \chi_{BH} \mathbf{W}_{H,p}^q + \mathbf{V}_E^{q-1} \quad (9a)$$

$$\mathbf{W}_H^{*q} - \chi_{AE} \mathbf{W}_E^{*q} = \chi_{BE} \mathbf{W}_{E,p}^q + \mathbf{V}_H^{q-1} \quad (9b)$$

$$\mathbf{W}_{E,p+1}^q - \chi_{BH} \mathbf{W}_{H,p+1}^q = \mathbf{W}_E^{*q} - \chi_{BH} \mathbf{W}_{H,p}^q \quad (9c)$$

$$\mathbf{W}_{H,p+1}^q - \chi_{BE} \mathbf{W}_{E,p+1}^q = \mathbf{W}_H^{*q} - \chi_{BE} \mathbf{W}_{E,p}^q \quad (9d)$$

Continuing to merge and tidy up equations (9a) ~ (9d), one can obtain

$$(\mathbf{I} - \chi_{AH} \chi_{AE}) \mathbf{W}_E^{*q} = \chi_{AH} \chi_{BE} \mathbf{W}_{E,p}^q + \chi_{BH} \mathbf{W}_{H,p}^q + \chi_{AH} \mathbf{V}_H^{q-1} + \mathbf{V}_E^{q-1} \quad (10a)$$

$$(\mathbf{I} - \chi_{BH} \chi_{BE}) \mathbf{W}_E^{*q} = (\mathbf{I} + \chi_{BH} \chi_{AE}) \mathbf{W}_E^{*q} - \chi_{BH} \mathbf{W}_{H,p}^q + \chi_{BH} \mathbf{V}_H^{q-1} \quad (10b)$$

$$\mathbf{W}_{H,p+1}^q = \chi_{BE} \mathbf{W}_{E,p+1}^q + \chi_{AE} \mathbf{W}_E^{*q} + \mathbf{V}_H^{q-1} \quad (10c)$$

Substituting the corresponding coefficient matrixes into equations (10a) ~ (10c), the FDTD expanding forms for the iteration calculation of the proposed method are obtained.

$$\begin{aligned} & (1 + ab(m^2/\rho^2)) e_{\rho}^{*q} \\ & = \mp ab(m/\rho)(\partial/\partial\rho + 1/\rho) e_{\varphi,p}^q - a(\partial/\partial z) h_{\varphi,p}^q \\ & \mp 2a(m/\rho) \sum_{k=0}^{q-1} h_z^k - 2 \sum_{k=0}^{q-1} e_{\rho}^k \end{aligned} \quad (11a)$$

$$\begin{aligned} e_{\varphi}^{*q} & = ab(\partial/\partial\rho)(\partial/\partial\rho + 1/\rho) e_{\varphi,p}^q + a(\partial/\partial z) h_{\rho,p}^q \\ & + 2a(\partial/\partial\rho) \sum_{k=0}^{q-1} h_z^k - 2 \sum_{k=0}^{q-1} e_{\varphi}^k \pm ab(\partial/\partial\rho)(m/\rho) e_{\rho}^{*q} \end{aligned} \quad (11b)$$

$$\begin{aligned} & (1 + ab(m^2/\rho^2)) e_z^{*q} \\ & = \mp ab(m/\rho)(\partial/\partial z) e_{\varphi,p}^q + a(\partial/\partial\rho + 1/\rho) h_{\varphi,p}^q \\ & \pm 2a(m/\rho) \sum_{k=0}^{q-1} h_{\rho}^k - 2 \sum_{k=0}^{q-1} e_z^k \end{aligned} \quad (11c)$$

$$\begin{aligned} & (1 - ab(\partial/\partial z)^2) e_{\rho,p+1}^q \\ & = e_{\rho}^{*q} - ab(\partial/\partial z)(\partial/\partial\rho) e_z^{*q} + a(\partial/\partial z) h_{\varphi,p}^q \\ & + 2a(\partial/\partial z) \sum_{k=0}^{q-1} h_{\varphi}^k \end{aligned} \quad (11d)$$

$$\begin{aligned} & (1 - ab(\partial/\partial z)^2) e_{\varphi,p+1}^q \\ & = e_{\varphi}^{*q} \pm ab(\partial/\partial z)(m/\rho) e_z^{*q} - a(\partial/\partial z) h_{\rho,p}^q \\ & - 2a(\partial/\partial z) \sum_{k=0}^{q-1} h_{\rho}^k \end{aligned} \quad (11e)$$

$$\begin{aligned} e_{z,p+1}^q & = e_z^{*q} + ab(\partial/\partial\rho + 1/\rho)(\partial/\partial\rho) e_z^{*q} \\ & - ab(\partial/\partial\rho + 1/\rho) h_{\varphi,p}^q - 2a(\partial/\partial\rho + 1/\rho) \sum_{k=0}^{q-1} h_{\varphi}^k \\ & - ab(\partial/\partial\rho + 1/\rho)(\partial/\partial z) e_{\rho,p+1}^q \end{aligned} \quad (11f)$$

$$h_{\rho,p+1}^q = b(\partial/\partial z) e_{\varphi,p+1}^q \pm b(m/\rho) e_z^{*q} - 2 \sum_{k=0}^{q-1} h_{\rho}^k \quad (11g)$$

$$h_{\varphi,p+1}^q = -b(\partial/\partial z) e_{\rho,p+1}^q + b(\partial/\partial\rho) e_z^{*q} - 2 \sum_{k=0}^{q-1} h_{\varphi}^k \quad (11h)$$

$$h_{z,p+1}^q = -b(\partial/\partial\rho + 1/\rho) e_{\varphi,p+1}^q \mp b(m/\rho) e_{\rho}^{*q} - 2 \sum_{k=0}^{q-1} h_z^k \quad (11i)$$

Similar to the initial value calculation process, the iteration calculation has only two tri-diagonal equations. Thus, the efficiency of the iterative calculation in the proposed method is definitely better than the existing one.

$$\begin{aligned} & \left(- (ab/(\Delta z)^2) (e_{\rho}^q(i+1/2, j-1) + e_{\rho}^q(i+1/2, j+1)) \right) \\ & \left(+ (1 + 2ab/(\Delta z)^2) e_{\rho}^q(i+1/2, j) \right) \\ & = e_{\rho}^{*q}(i+1/2, j) - (ab/(\Delta z \Delta \rho)) \begin{bmatrix} e_z^{*q}(i+1, j+1/2) \\ -e_z^{*q}(i, j+1/2) \\ -e_z^{*q}(i+1, j-1/2) \\ +e_z^{*q}(i, j-1/2) \end{bmatrix} \end{aligned} \quad (12)$$

Finally, the first order FDTD central difference expansion of the equations (6d) is given. The first order FDTD central difference expansion way of others is similar with formula (12).

D. SPECIAL TREATMENT FOR FIELD COMPONENTS ON Z-AXIS

When the 3-D cylindrical coordinate structure is a purely symmetric body, it can be transformed into a 2-D space for calculation. The transformation processing is shown from (a) to (b) of FIGURE 2.

As shown in the (b) of the FIGURE 2, when $\rho = 0$, every electromagnetic field components e_z , e_{φ} and h_{ρ} on the axis have mathematical strangeness, which should be specially treated. The schemes of discussion in [11] and [13] is that only e_z components need to be specially treated at $\rho = 0$ for $m = 0$. However, the above special treating schemes for field components on the axis are not necessarily applicable to the proposed method in this paper. Next, we will make a concrete analysis for the treatment of electromagnetic field components on the axis in the proposed method.

As shown in (b) of the FIGURE 2, there are electromagnetic field components $e_z(0, j+1/2)$, $e_{\varphi}(0, j)$ and $h_{\rho}(0, j+1/2)$ on the axis. Therefore, we need to determine that whether $e_z^{*q}(0, j+1/2)$, $e_z^q(0, j+1/2)$, $e_{\varphi}^{*q}(0, j)$, $e_{\varphi}^q(0, j)$,

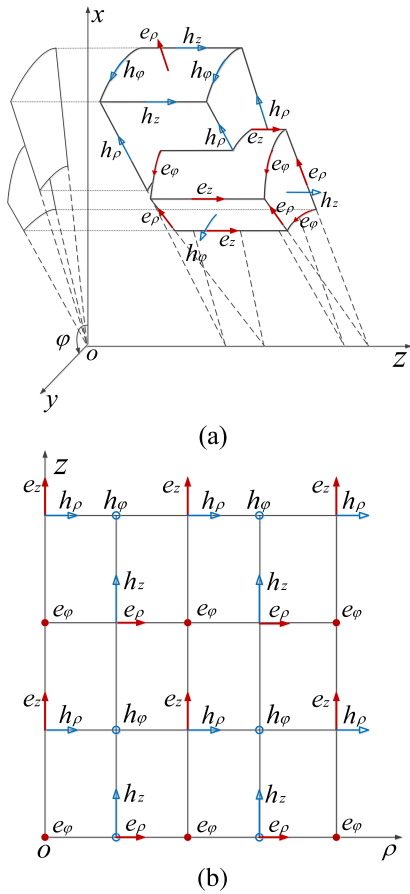


FIGURE 2. The realization principle of transforming 3-D problem into 2-D space. 3-D problems are projected into 2-D space. (b) Distribution of the field components around the axis in BOR system.

\$h_\rho^q(0, j + 1/2)\$ are used in the initial value calculation equations (6a) ~ (6i) and the iterative calculation (11a) ~ (11i) of the proposed method. FIGURE 3 is the analysis for the electromagnetic field components on the axis of the proposed method. Clearly, the electric field component \$e_z^{*q}(0, j + 1/2)\$ on the axis only needs to be specially treated in the initial value calculation and the iteration calculation of the proposed method, respectively.

In [13], the treatment scheme for the field component on the axis has been discussed. The equation \$e_z^{*q}(0, j + 1/2)\$ at \$\rho = 0\$ can be directly obtained.

$$e_z^{*q}(0, j + 1/2) = (4a/\Delta\rho) h_\phi^q(1/2, j + 1/2) - 2 \sum_{k=0}^{q-1} e_z^k(0, j + 1/2) \quad (13)$$

Expanding (6h) and (11h) at \$\rho = 0\$, one can obtain

$$h_\phi^q(1/2, j + 1/2) + 2 \sum_{k=0}^{q-1} h_\phi^k(1/2, j + 1/2) = (b/\Delta\rho) [e_z^{*q}(1, j + 1/2) - e_z^{*q}(0, j + 1/2)] - (b/\Delta z) [e_\rho^q(1/2, j + 1) - e_\rho^q(1/2, j)] \quad (14)$$

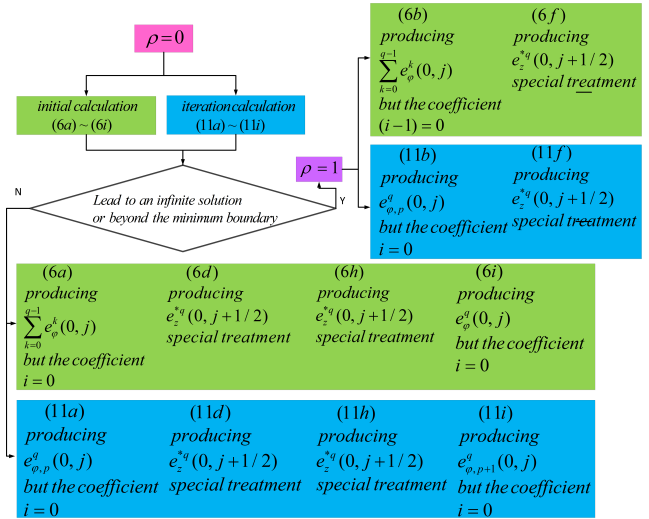


FIGURE 3. The analysis for the field components on the axis.

$$h_{\phi, p+1}^q(1/2, j + 1/2) + 2 \sum_{k=0}^{q-1} h_\phi^k(1/2, j + 1/2) = (b/\Delta\rho) [e_z^{*q}(1, j + 1/2) - e_z^{*q}(0, j + 1/2)] - (b/\Delta z) [e_{\rho, p+1}^q(1/2, j + 1) - e_{\rho, p+1}^q(1/2, j)] \quad (15)$$

Substituting equations (14) and (15) into equation (13), one can obtain the treatment equations on the axis for the initial value calculation and the iteration calculation, respectively.

$$\begin{aligned} & \left(\begin{array}{c} (1 + 4ab/(\Delta\rho^2)) e_z^{*q}(0, j + 1/2) \\ -4ab/(\Delta\rho^2) e_z^{*q}(1, j + 1/2) \end{array} \right) \\ & = -4ab/(\Delta\rho\Delta z) [e_\rho^q(1/2, j + 1) - e_\rho^q(1/2, j)] \\ & \quad - (8a/\Delta\rho) \sum_{k=0}^{q-1} h_\phi^k(1/2, j + 1/2) - 2 \sum_{k=0}^{q-1} e_z^k(0, j + 1/2) \quad (16) \\ & \left(\begin{array}{c} (1 + 4ab/(\Delta\rho^2)) e_z^{*q}(0, j + 1/2) \\ -4ab/(\Delta\rho^2) e_z^{*q}(1, j + 1/2) \end{array} \right) \\ & = -4ab/(\Delta\rho\Delta z) [e_{\rho, p+1}^q(1/2, j + 1) - e_{\rho, p+1}^q(1/2, j)] \\ & \quad - (8a/\Delta\rho) \sum_{k=0}^{q-1} h_\phi^k(1/2, j + 1/2) - 2 \sum_{k=0}^{q-1} e_z^k(0, j + 1/2) \quad (17) \end{aligned}$$

III. THE EXPLICIT CALCULATION SCHEME AT Z-DIRECTION

Previously, the principle of the proposed method based on \$\rho\$-direction explicit calculation was introduced. Here, in order to reflect the flexibility and variability of the proposed method in this paper, we provide a z-direction explicit calculation scheme. Their coefficient matrixes are shown as follows.

$$A' = \begin{bmatrix} 0 & X'_{AH} \\ X'_{AE} & 0 \end{bmatrix}, \quad B' = \begin{bmatrix} 0 & X'_{BH} \\ X'_{BE} & 0 \end{bmatrix},$$

$$\begin{aligned} \chi'_{AH} &= \begin{bmatrix} 0 & -a(\partial/\partial z) & 0 \\ 0 & 0 & -a(\partial/\partial \rho) \\ 0 & a(\partial/\partial \rho + 1/\rho) & 0 \end{bmatrix}, \\ \chi'_{AE} &= \begin{bmatrix} 0 & b(\partial/\partial z) & 0 \\ 0 & 0 & b(\partial/\partial \rho) \\ 0 & -b(\partial/\partial \rho + 1/\rho) & 0 \end{bmatrix}, \\ \chi'_{BH} &= \begin{bmatrix} 0 & 0 & a(\pm m/\rho) \\ a(\partial/\partial z) & 0 & 0 \\ -a(\pm m/\rho) & 0 & 0 \end{bmatrix}, \\ \chi'_{BE} &= \begin{bmatrix} 0 & 0 & -b(\mp m/\rho) \\ -b(\partial/\partial z) & 0 & 0 \\ b(\mp m/\rho) & 0 & 0 \end{bmatrix}, \end{aligned}$$

Note that a and b are same with the ρ -direction one.

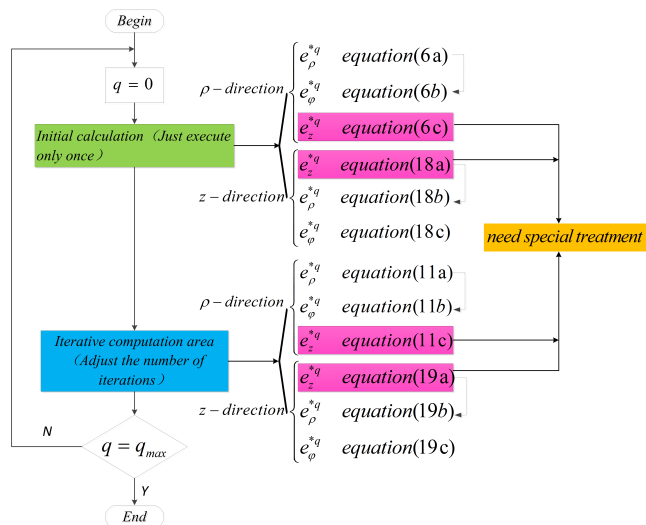


FIGURE 4. The whole execution process of the z-direction explicit calculation scheme.

The principle of realization for z-direction explicit calculation scheme is similar with ρ -direction one, The difference between the both schemes is that the former one, e_z^{*q} needs to be firstly explicit calculated and the latter one, e_ρ^{*q} needs to be firstly explicit calculated. The specific difference between the both schemes is shown in FIGURE 4. Thus, the FDTD expanding forms of the z-direction explicit calculation scheme can be directly obtained.

$$\begin{aligned} &(1 - ab(\partial/\partial \rho + 1/\rho)(\partial/\partial \rho)) e_z^{*q} \\ &= 2ab(\partial/\partial \rho + 1/\rho)(\partial/\partial z) \sum_{k=0}^{q-1} e_\rho^k - 2 \sum_{k=0}^{q-1} e_z^k \\ &\quad \pm 2a(m/\rho) \sum_{k=0}^{q-1} h_\rho^k - 2a(\partial/\partial \rho + 1/\rho) \sum_{k=0}^{q-1} h_\phi^k \end{aligned} \quad (18a)$$

$$\begin{aligned} e_\rho^{*q} &= -ab(\partial/\partial z)(\partial/\partial \rho) e_z^{*q} - 2 \sum_{k=0}^{q-1} e_\rho^k \\ &\quad - 2ab(\partial/\partial z)^2 \sum_{k=0}^{q-1} e_\rho^k + 2a(\partial/\partial z) \sum_{k=0}^{q-1} h_\phi^k \\ &\quad \pm 2a(m/\rho) \sum_{k=0}^{q-1} h_z^k \end{aligned} \quad (18b)$$

$$\begin{aligned} &(1 - ab(\partial/\partial \rho)(\partial/\partial \rho + 1/\rho)) e_\phi^{*q} \\ &= \mp 2ab(\partial/\partial \rho)(m/\rho) \sum_{k=0}^{q-1} e_\rho^k - 2 \sum_{k=0}^{q-1} e_\phi^k \\ &\quad - 2a(\partial/\partial z) \sum_{k=0}^{q-1} h_\rho^k + 2a(\partial/\partial \rho) \sum_{k=0}^{q-1} h_z^k \end{aligned} \quad (18c)$$

$$\begin{aligned} &(1 + ab(m^2/\rho^2)) e_\rho^q \\ &= e_\rho^{*q} \pm ab(m/\rho)(\partial/\partial \rho + 1/\rho) e_\phi^{*q} \end{aligned} \quad (18d)$$

$$e_\phi^q = \pm ab(\partial/\partial z)(m/\rho) e_z^q + (1 + ab(\partial/\partial z)^2) e_\phi^{*q} \quad (18e)$$

$$\begin{aligned} &(1 + ab(m^2/\rho^2)) e_z^q \\ &= e_z^{*q} \pm ab(m/\rho)(\partial/\partial z) e_\phi^{*q} \end{aligned} \quad (18f)$$

$$h_\rho^q = b(\partial/\partial z) e_\phi^{*q} \pm b(m/\rho) e_z^q - 2 \sum_{k=0}^{q-1} h_\rho^k \quad (18g)$$

$$h_\phi^q = b(\partial/\partial \rho) e_z^{*q} - b(\partial/\partial z) e_\rho^q - 2 \sum_{k=0}^{q-1} h_\phi^k \quad (18h)$$

$$h_z^q = -b(\partial/\partial \rho + 1/\rho) e_\phi^{*q} \pm b(m/\rho) e_\rho^q - 2 \sum_{k=0}^{q-1} h_z^k \quad (18i)$$

$$\begin{aligned} &(1 - ab(\partial/\partial \rho + 1/\rho)(\partial/\partial \rho)) e_z^{*q} \\ &= -ab(\partial/\partial \rho + 1/\rho)(\partial/\partial z) e_{\rho,p}^q - 2 \sum_{k=0}^{q-1} e_z^k \\ &\quad \mp a(m/\rho) h_{\rho,p}^q - 2a(\partial/\partial \rho + 1/\rho) \sum_{k=0}^{q-1} h_\phi^k \end{aligned} \quad (19a)$$

$$\begin{aligned} e_\rho^{*q} &= -ab(\partial/\partial z)(\partial/\partial \rho) e_z^{*q} - 2 \sum_{k=0}^{q-1} e_\rho^k + ab(\partial/\partial z)^2 e_{\rho,p}^q \\ &\quad \pm a(m/\rho) h_{z,p}^q + 2a(\partial/\partial z) \sum_{k=0}^{q-1} h_\phi^k \end{aligned} \quad (19b)$$

$$\begin{aligned} &(1 - ab(\partial/\partial \rho)(\partial/\partial \rho + 1/\rho)) e_\phi^{*q} \\ &= \pm ab(\partial/\partial \rho)(m/\rho) e_{\rho,p}^q - 2 \sum_{k=0}^{q-1} e_\phi^k \\ &\quad + a(\partial/\partial z) h_{\rho,p}^q + 2a(\partial/\partial \rho) \sum_{k=0}^{q-1} h_z^k \end{aligned} \quad (19c)$$

$$\begin{aligned} &(1 + ab(m^2/\rho^2)) e_{\rho,p+1}^q \\ &= e_\rho^{*q} \mp ab(m/\rho)(\partial/\partial \rho + 1/\rho) e_\phi^{*q} \\ &\quad \mp a(m/\rho) h_{z,p}^q \mp 2a(m/\rho) \sum_{k=0}^{q-1} h_z^k \end{aligned} \quad (19d)$$

$$\begin{aligned} e_{\phi,p+1}^q &= \pm ab(\partial/\partial z)(m/\rho) e_{z,p+1}^q + (1 + ab(\partial/\partial z)^2) e_\phi^{*q} \\ &\quad - a(\partial/\partial z) h_{\rho,p}^q - 2a(\partial/\partial z) \sum_{k=0}^{q-1} h_\rho^k \end{aligned} \quad (19e)$$

$$\begin{aligned} & \left(1 + ab(m^2/\rho^2)\right) e_{z,p+1}^q \\ & = e_{z,p+1}^{*q} \mp ab(m/\rho)(\partial/\partial z)e_{\rho,p}^{*q} \\ & \quad \pm a(m/\rho)h_{\rho,p}^q \pm 2a(m/\rho) \sum_{k=0}^{q-1} h_{\rho}^k \end{aligned} \quad (19f)$$

$$h_{\rho,p+1}^q = b(\partial/\partial z)e_{\rho,p}^{*q} \pm b(m/\rho)e_{z,p+1}^q - 2 \sum_{k=0}^{q-1} h_{\rho}^k \quad (19g)$$

$$h_{\varphi,p+1}^q = b(\partial/\partial \rho)e_{z,p+1}^{*q} - b(\partial/\partial z)e_{\rho,p+1}^q - 2 \sum_{k=0}^{q-1} h_{\varphi}^k \quad (19h)$$

$$h_{z,p+1}^q = -b(\partial/\partial \rho + 1/\rho)e_{\varphi,p+1}^{*q} \pm b(m/\rho)e_{\rho,p+1}^q - 2 \sum_{k=0}^{q-1} h_z^k \quad (19i)$$

IV. CONVERGENCE ANALYSIS AND STABILITY PROOF FOR ITERATIVE CALCULATION

The convergence condition of ρ -direction scheme can be proved by theoretical analysis method and numerical calculation. By referring to the analysis methods in [18], [20], and [22], we can directly obtain the convergence conditions through equation (8).

A. DERIVATION OF CONVERGENCE CONDITION

In the cylindrical coordinate system, six electric- and magnetic-field components in the spectral domain can always be expressed as

$$E_{\rho}^q = e_{\rho}^q f(\rho, \varphi, z) \quad (20a)$$

$$\tilde{E}_{\varphi}^q = \rho e_{\varphi}^q f(\rho, \varphi, z) \quad (20b)$$

$$E_z^q = e_z^q f(\rho, \varphi, z) \quad (20c)$$

$$H_{\rho}^q = h_{\rho}^q f(\rho, \varphi, z) \quad (20d)$$

$$\tilde{H}_{\varphi}^q = \rho h_{\varphi}^q f(\rho, \varphi, z) \quad (20e)$$

$$H_z^q = h_z^q f(\rho, \varphi, z) \quad (20f)$$

where $f(\rho, \varphi, z) = B_m(\varsigma_{\rho}\rho)e^{\vec{j}m\varphi}e^{\vec{j}\varsigma_z z}$, $\vec{j} = \sqrt{-1}$, B_m is the appropriate Bessel function, ς_{ρ} and ς_z are the spatial frequencies along the ρ - and z -directions, respectively. By substituting the earlier expressions into (7) and defining $\tilde{e}_{\varphi}^{*q} = \rho e_{\varphi}^{*q}$, $\tilde{e}_{\varphi,p+1}^q = \rho e_{\varphi,p+1}^q$, $\tilde{h}_{\varphi}^{*q} = \rho h_{\varphi}^{*q}$ and $\tilde{h}_{\varphi,p+1}^q = \rho h_{\varphi,p+1}^q$. Thus, the coefficient matrixes of equation (8) should be rewritten as

$$\Lambda_1 = \begin{bmatrix} & & & 0 & 0 & S_m/\rho \\ & 0 & & 0 & 0 & -\rho S_{\rho} \\ & & & -S_m/\rho & 0 & 0 \\ 0 & 0 & S_m/\rho & & & \\ 0 & 0 & \rho S_{\rho} & & & 0 \\ -S_m/\rho & 0 & 0 & & & \end{bmatrix},$$

$$\Lambda_2 = \begin{bmatrix} & & & 0 & -j(S_z/\rho) & 0 \\ & & & j(\rho S_z) & 0 & 0 \\ & & & 0 & S_{\rho}/\rho & 0 \\ 0 & j(S_z/\rho) & 0 & & & \\ -j(\rho S_z) & 0 & 0 & & & 0 \\ 0 & -S_{\rho}/\rho & 0 & & & \end{bmatrix}.$$

where $S_{\rho} = (2c/s)(B_m^{i+1/2} - B_m^{i-1/2})/(\Delta\rho B_m i)$, $S_m = \pm(2c/s)m$, $S_z = (4c/s)(\sin(\varsigma_z \Delta z)/\Delta z)$. Λ_1 and Λ_2 are the coefficient matrixes of the left side of the equations (8a) and (8b) respectively. In fact, Λ_1 and Λ_2 are another forms of A and B of the equation (7), thus, we can obtain the growth-share matrix of the iteration equation (7).

$$\Lambda = (I - B)^{-1}(I - A)^{-1}AB \quad (21)$$

According to the matrix theory, When all the eigenvalues $|\lambda| \leq 1$ of Λ , the iteration equation (7) is convergent. And then, the equation (21) can be modified as

$$\Lambda = (I - B)^{-1} [f(A)f(B)](I - B) \quad (22)$$

where $f(A) = (I - A)^{-1}A$, $f(B) = (I - B)^{-1}B$.

Obviously, Λ and $f(A)f(B)$ are similar matrices, thus, they have the same eigenvalue. The eigenvalue λ is satisfied with

$$\|\lambda\| \leq \|f(A)f(B)\| \leq \|f(A)\| \|f(B)\| \quad (23)$$

When the eigenvalue $|\lambda_{A-max}| \leq 1$ of $\|f(A)\|$ and the eigenvalue $|\lambda_{B-max}| \leq 1$ of $\|f(B)\|$, the iterative calculation of the proposed method is convergent.

For example, according to the matrix theory, one can obtain

$$\|f(A)\|^2 = \lambda \left(f(A)f(A)^H \right)_{max} \quad (24)$$

where $f(A)^H$ is the associate matrix of $f(A)$, λ_{max} is the maximum eigenvalue.

Matlab calculation results show that the eigenvalues of $f(A)f(A)^H$ and $f(B)f(B)^H$ are

$$\lambda_{A-1,2} = 0 \quad (25a)$$

$$\lambda_{A-3,4} = \left(S_{\rho}^2 \rho^4 + S_m^2 \right) / \left(S_m^2 + \rho^2 \right) \quad (25b)$$

$$\lambda_{A-5,6} = S_m^2 / \left(S_m^2 + \rho^2 \right) \quad (25c)$$

$$\lambda_{B-1,2} = 0 \quad (26a)$$

$$\lambda_{A-3,4} = \lambda_{A-5,6} = \left(N \pm \sqrt{N^2 - 2\rho^2 S_z^2 (S_{\rho}^2 + S_z^2)^2 M} \right) / M \quad (26b)$$

where

$$\begin{aligned} N &= S_{\rho}^2 + S_z^2 + \rho^4 S_z^2 + 2\rho^2 S_z^4 + \rho^2 S_{\rho}^2 S_z^2, \\ M &= 2 \left(\rho^2 S_z^4 + 2\rho^2 S_z^2 + \rho^2 \right). \end{aligned}$$

Referring to the analysis process in [22], one can obtain $1 \geq 4c\rho/s\Delta\rho$ and $1 \geq 4c\rho/s\Delta z$. Thus, the convergence condition for the iteration calculation of the proposed method is $s \geq 4c\rho/\min(\Delta\rho, \Delta z)$.

B. PROOF OF STABILITY

The numerical method is used to prove the stability of the proposed method [20], [23]. The stability of the iterative calculation is illustrated by the long time oscillation of the time domain waveform. Therefore, an example of a resonator is used. In fact, the base function of WLP technology will attenuate with the increase of calculation time, therefore, when WLP technology is used to calculate the example of resonator, it will be difficult to calculate that is caused by the long calculation time.

In order to accurately calculate the resonator of the proposed method, the time-domain segmentation technology is adopted [20], [24]. Taking the conventional WLP BOR-FDTD as an example, the equations of the conventional WLP BOR-FDTD based on time-domain segmentation technology are

$$e_{\rho}^q + 2 \sum_{k=0}^{q-1} e_{\rho}^k = (2/s\varepsilon) (\pm(m/\rho)h_z^q - (\partial/\partial z)h_{\varphi}^q) + (2/s)E_{\rho}^{bef} \quad (26a)$$

$$e_{\varphi}^q + 2 \sum_{k=0}^{q-1} e_{\varphi}^k = (2/s\varepsilon) ((\partial/\partial z)h_{\rho}^q - (\partial/\partial \rho)h_z^q) + (2/s)E_{\varphi}^{bef} \quad (26b)$$

$$e_z^q + 2 \sum_{k=0}^{q-1} e_z^k = (2/s\varepsilon) (\partial(\rho h_{\varphi}^q)/\rho \partial \rho \mp (m/\rho)h_{\rho}^q) + (2/s)E_z^{bef} \quad (26c)$$

$$h_{\rho}^q + 2 \sum_{k=0}^{q-1} h_{\rho}^k = (2/s\mu) ((\partial/\partial z)e_{\varphi}^q \pm (m/\rho)e_z^q) + (2/s)H_{\rho}^{ref} \quad (26d)$$

$$h_{\varphi}^q + 2 \sum_{k=0}^{q-1} h_{\varphi}^k = (2/s\mu) ((\partial/\partial \rho)e_z^q - (\partial/\partial z)e_{\rho}^q) + (2/s)H_{\varphi}^{ref} \quad (26e)$$

$$h_z^q + 2 \sum_{k=0}^{q-1} h_z^k = (2/s\mu) (-\partial(\rho e_{\varphi}^q)/\rho \partial \rho \mp (m/\rho)e_{\rho}^q) + (2/s)H_z^{ref} \quad (26f)$$

where E_i^{bef} , H_i^{ref} , $i = \rho, \varphi, z$ are the electromagnetic field components at the last time point, which are calculated by the previous period.

Obviously, the new equations (27) are formed by adding E_i^{bef} and H_i^{ref} to the right side of the conventional WLP BOR-FDTD. In the similar way, we can obtain the new equations of the proposed method based on time-domain segmentation technology by adding E_i^{bef} and H_i^{ref} to the right side of equations (6) and (11), not tired in words here.

In order to verify the stability of the proposed method, an perfectly electrically conducting (PEC) cavity resonator is computed. The radius and height of the cavity are both 11cm. The computational domain is meshed using a uniform grid with $\Delta\rho = \Delta z = 1\text{cm}$, $s = 1.0 \times 10^{11}$, $q = 500$ and Nt is

the number of iterations. The total calculation time is 260ns which is divided into 13 periods for calculation and every 20ns is a period of time. On the premise that the convergence condition is $s \geq 4c\rho/\min(\Delta\rho, \Delta z)$, the proposed method compares with the conventional WLP BOR-FDTD method. The results are shown in (a) and (b) of FIGURE 5.

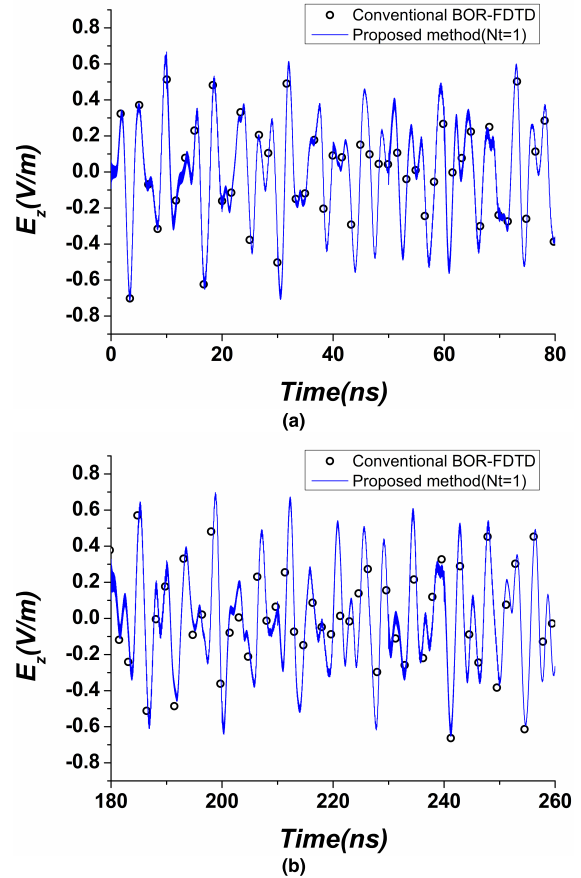


FIGURE 5. Computational results of conventional WLP BOR-FDTD method and the proposed method. (a) 0~80ns. (b) 180~260ns.

The (a) and (b) in FIGURE 5 show an excellent agreement between conventional WLP BOR-FDTD method and the proposed method. Thus, the proposed method is stable under $s \geq 4c\rho/\min(\Delta\rho, \Delta z)$. In fact, $s = 2 \times 10^{10}$ is the minimum stability condition in this cavity resonator example, if $s < 2 \times 10^{10}$, the numerical result is divergent. Therefore, we can determine that $s \geq 4c\rho/\min(\Delta\rho, \Delta z)$ is not only the convergence condition but also the stability condition of the proposed method at ρ -direction explicit calculation.

V. TWO SCATTERING NUMERICAL RESULTS AND ANALYSES

In order to verify the proposed method, two scattering numerical examples for ρ -direction and z -direction are given.

First example, a single groove scattered model is given for verifying the ρ -direction calculation of the proposed method. The depth of the groove is 2cm. The obliquely incident plane wave is added through Huygen's surface at $\rho = 22.5\text{cm}$ and

$z = \pm 22.5\text{cm}$, and the incident angle is $\theta_i = 45^\circ$, as shown in FIGURE 6. The incident electric field is

$$E_i(t) = E_0 \cos(2\pi f_0 t) \exp\left(-4\pi \left(\frac{t - t_0}{\tau}\right)^2\right) \quad (27)$$

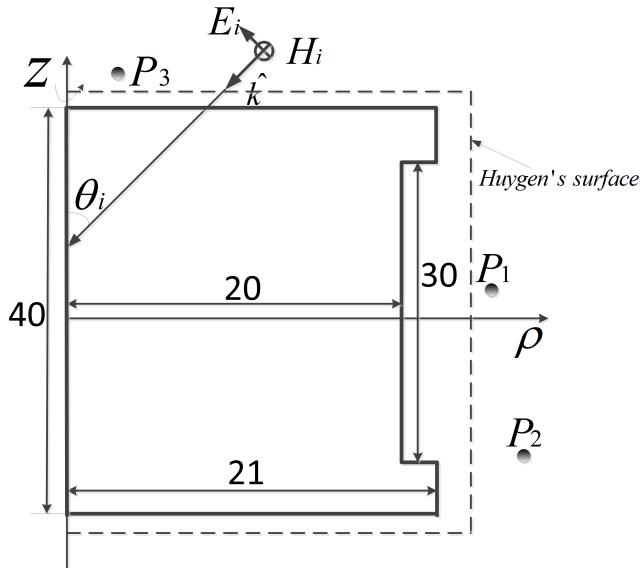


FIGURE 6. Illustration of the irregular cylinder under oblique incident wave.

where $E_0 = 1000\text{V/m}$, $f_0 = 10\text{GHz}$, $\tau = 1.5/f_0$, $t_0 = 1.75/f_0$. In addition, choose $s = 8 \times 10^{11}$, $q = 210$ for comparing with the existing efficient WLP-based BOR-FDTD method [19], and the range of mis from 0 to 14. The computational domain is meshed using a uniform grid with $\Delta\rho = 2\Delta z = 0.2\text{cm}$, leading to the total mesh of 100×200 , and the first order Mur absorbing boundary condition is used to truncate the boundary [25].

The simulated electric field are E_z components at point $P1(48, 0)$ and $P2(60, -39)$. The iterations of the whole computational domain and local area are denoted by Nt and $Np1$, respectively. And the size of the local computational area is $10\Delta\rho \times 90\Delta z$ for nearing the groove.

In addition, to demonstrate the better efficiency of the proposed algorithm comparing with the existing algorithm, an error formulation is provided, which is defined as

$$E_{z,error} = \log |E_z(t) - E_{z,BOR-FDTD}(t)| \quad (28)$$

where $E_z(t)$ are the simulation data about electric field of the one-step WCS BOR-FDTD method [18], the existing efficient WLP-based BOR-FDTD method [19] and the proposed method, $E_{z,BOR-FDTD}(t)$ is the electric field datum of the conventional BOR-FDTD method.

By using conventional BOR-FDTD method, the one-step WCS BOR-FDTD method, the existing efficient WLP-based BOR-FDTD method and the proposed method, the time-domain field waveforms at the observation points $P1$ and $P2$ are shown in FIGURES 7-8. The numerical results show an excellent agreement between the proposed method and the conventional BOR-FDTD method.

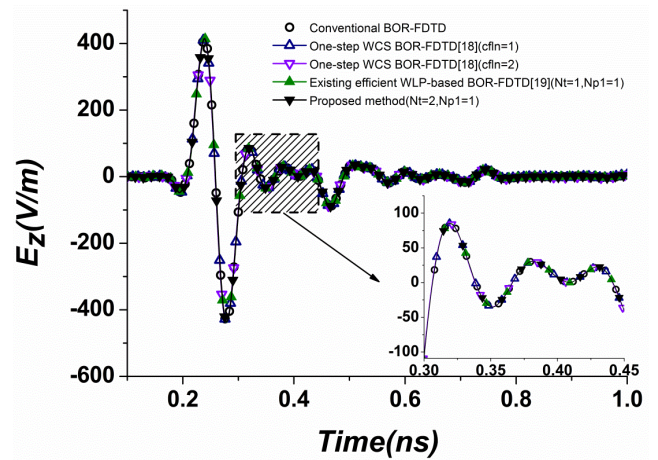


FIGURE 7. Computational results E_z at point $P1$ of the proposed method and existing BOR-FDTD methods.

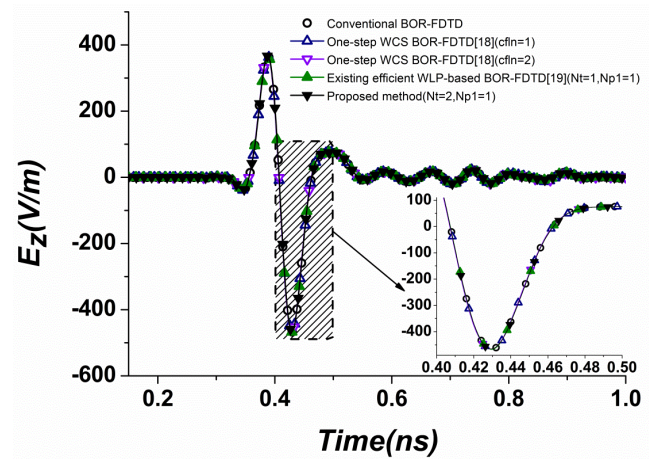


FIGURE 8. Computational results E_z at point $P2$ of the proposed method and existing BOR-FDTD methods.

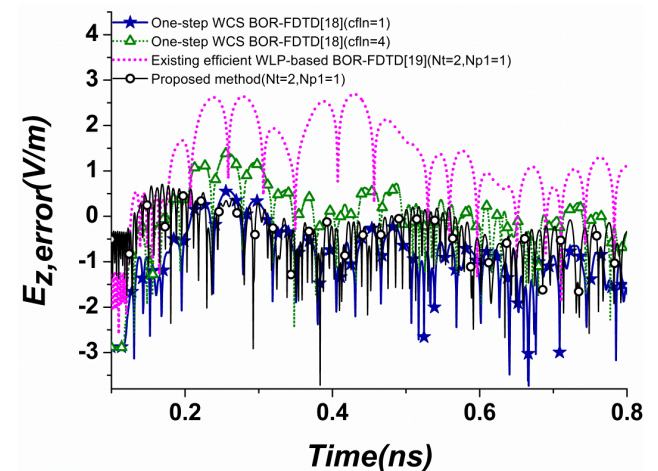


FIGURE 9. Errors obtained by E_z at point $P1$ of the proposed method and existing BOR-FDTD methods.

FIGURE 9 and FIGURE 10 give the errors which are obtained by E_z at the observation points $P1$ and $P2$ of the proposed method ($Nt = 2, Np1 = 1$), the one-step WCS BOR-FDTD method ($cfln = 1$ and 4) and the

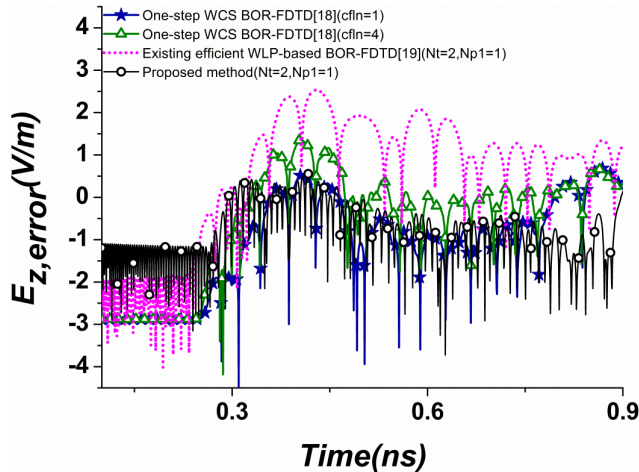


FIGURE 10. Errors obtained by E_z at point P_2 of the proposed method and existing BOR-FDTD methods.

existing efficient WLP-based BOR-FDTD method ($N_t = 2, N_{p1} = 1$). The error results show that the accuracies of the proposed method ($N_t = 2, N_{p1} = 1$) and the one-step WCS BOR-FDTD method ($cfln = 1$) are almost equal. However, the CPU time are 61s and 418s respectively. Namely, the proposed method can be raised the efficiency almost 85% than the one-step WCS BOR-FDTD method ($cfln = 1$). The accuracy of the proposed method ($N_t = 2, N_{p1} = 1$) can be raised almost 61% than the one-step WCS BOR-FDTD method ($cfln = 4$) and almost 69% than the existing efficient WLP-based BOR-FDTD method ($N_t = 2, N_{p1} = 1$) respectively. Meanwhile, the memory of the proposed method can be declined almost 45% than the one-step WCS BOR-FDTD method and almost 5% than the existing efficient WLP-based BOR-FDTD method, as shown in TABLE 1 which includes the CUP time and memory of these existing BOR-FDTD methods.

In a word, the simulation results of the first example show that the combination of the explicit ideology and WLP technology can improve the computational efficiency and accuracy for the BOR system in different degrees by comparing the existing BOR -FDTD methods and greatly reduce the consumption of memory. In other words, this proposed method not only solves the problem of time step limitation and large memory consumption, but also greatly improves the computational efficiency, accuracy and memory consumption of calculation.

Second example, the scattered model shown in FIGURE 6 is still used to verify the performance of the z -direction explicit calculation. The computational domain is meshed using a uniform grid with $2\Delta\rho = \Delta z = 0.2\text{cm}$, the local area is denoted by N_{p2} . And the size of the local computational area is $10\Delta\rho \times 200\Delta z$ for nearing the axis. The simulated electric field is $P3(5, 48)$, the other conditions are same with the first example.

FIGURE 11 shows the results of the proposed method with axis treating and no axis treating compared with the

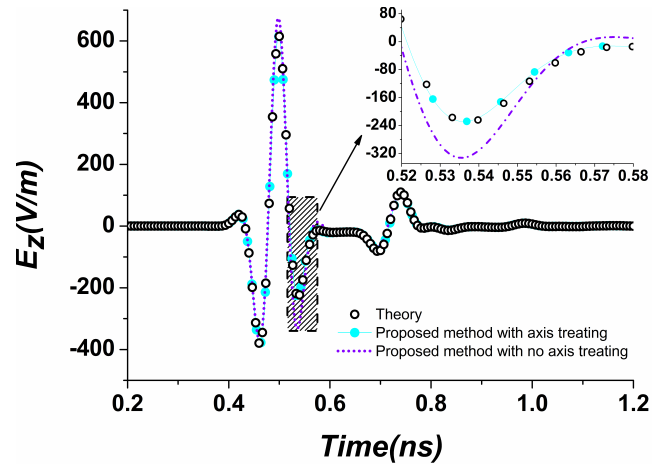


FIGURE 11. Computational results E_z at point P_3 of the proposed method with axis treating.

theoretical result at $P3$. Clearly, the numerical result shows an excellent agreement between the axis treating of the proposed method and the theoretical result. Namely, the special treatment for the field components on axis in part II of this paper is verified from another perspective.

By using conventional BOR-FDTD method, the one-step WCS BOR-FDTD method, the existing efficient WLP-based BOR-FDTD method and the proposed method, the time-domain field waveforms at the observation point $P3$ are shown in FIGURES 12. The numerical results show an excellent agreement between the proposed method and the conventional BOR-FDTD method.

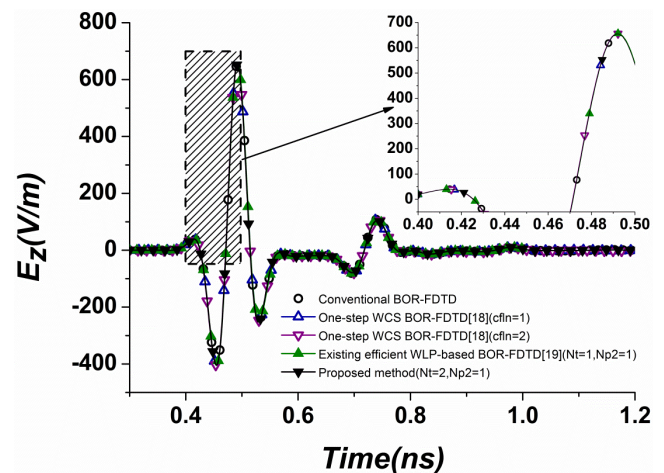


FIGURE 12. Computational results E_z at point P_3 of the proposed method and existing BOR-FDTD methods.

FIGURE 13 gives the errors which are obtained by E_z at the observation point $P3$ of the proposed method ($N_t = 2, N_{p2} = 1$), the one-step WCS BOR-FDTD method ($cfln = 1$ and 3) and the existing efficient WLP-based BOR-FDTD method ($N_t = 2, N_{p2} = 1$). The results are similar with the first example. The error of the proposed method

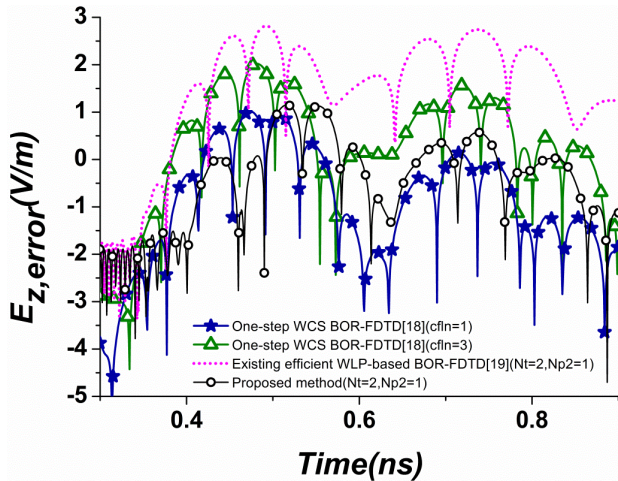


FIGURE 13. Errors obtained by E_z at point P_3 of the proposed method and existing BOR-FDTD methods.

($Nt = 2, Np2 = 1$) is almost equal with the one-step WCS BOR-FDTD method ($cfln = 1$). Comparing with the one-step WCS BOR-FDTD method ($cfln = 3$) and the existing efficient WLP-based BOR-FDTD method ($Nt = 2, Np2 = 1$), the accuracy can be raised almost 45% and 59%, respectively. Meanwhile, the computational efficiency and the memory consumption also can be greatly improved that can refer to the TABLE 1 for details, not tired in words here.

TABLE 1. CPU time and memory for different methods.

METHOD	Computational Condition	CPU Time	Memory
The proposed method	($Nt = 2, Np1 = 1$)	61s	19M
	($cfln = 1$)	418s	34M
The method in [18]	($cfln = 2$)	171s	34M
	($cfln = 4$)	95s	34M
	($cfln = 8$)	NAN	
	($Nt = 2, Np1 = 1$)	79s	20M
The method in [19]	($Nt = 3, Np1 = 2$)	106s	20M
	($Nt = 4, Np1 = 4$)	96s	20M

VI. CONCLUSION

In this work, a novel efficient weighted Laguerre polynomial (WLP)-based finite-difference time-domain (FDTD) method with explicit treating ideology is proposed. This proposed method is flexible and variable, explicit scheme at both ρ -direction and z -direction can be realized for the BOR system. By combining the explicit treating ideology and WLP technology, the limitation of time step Δt can be eliminated effectively and the original time domain problem can be converted into another one related to the time-scale factor s . Meanwhile, the consumption of memory can be greatly saved. Two scattering examples show that the proposed method can greatly improve the computational efficiency and

accuracy and weaken the cumbersomeness of Gauss-Seidel process, compared with the existing efficient WLP-based BOR-FDTD method and the one-step WCS BOR-FDTD method.

REFERENCES

- [1] W. C. Chew, M. Moghaddam, and E. Yannakakis, "Modeling of the subsurface interface radar," in *Proc. 11th Annu. Int. Symp. Geosci. Remote Sens.*, College Park, MD, USA, May 1990, p. 31.
- [2] S. Shi and D. W. Prather, "Electromagnetic analysis of axially symmetric diffractive optical elements illuminated by oblique incident plane waves," *J. Opt. Soc. Amer. A, Opt. Image Sci.*, vol. 18, no. 11, pp. 2901–2907, Nov. 2001.
- [3] D. W. Prather and S. Shi, "Formulation and application of the finite-difference time-domain method for the analysis of axially symmetric diffractive optical elements," *J. Opt. Soc. Amer. A, Opt. Image Sci.*, vol. 16, no. 5, pp. 1131–1142, May 1999.
- [4] Y. Chen, R. Mittra, and P. Harms, "Finite-difference time-domain algorithm for solving Maxwell's equations in rotationally symmetric geometries," *IEEE Trans. Microw. Theory Techn.*, vol. 44, no. 6, pp. 832–839, Jun. 1996.
- [5] W. Yu and R. Mittra, "A technique for improving the accuracy of the nonuniform finite-difference time-domain algorithm," *IEEE Trans. Microw. Theory Techn.*, vol. 47, no. 3, pp. 353–356, Mar. 1999.
- [6] D. B. Davidson and R. W. Ziolkowski, "Body-of-revolution finite-difference time-domain modeling of space-time focusing by a three dimensional," *J. Opt. Soc. Amer. A, Opt. Image Sci.*, vol. 11, no. 4, pp. 1471–1490, Apr. 1994.
- [7] A. Taflov and S. C. Hagness, *Computational Electrodynamics: The Finite-Difference Time-Domain Method*, 2nd ed. Boston, MA, USA: Artech House, 2000, pp. 109–174.
- [8] T. Namiki, "A new FDTD algorithm based on alternating-direction implicit method," *IEEE Trans. Microw. Theory Techn.*, vol. 47, no. 10, pp. 2003–2007, Oct. 1999.
- [9] C. Yuan and Z. Chen, "A three-dimensional unconditionally stable ADI-FDTD method in the cylindrical coordinate system," *IEEE Trans. Microw. Theory Techn.*, vol. 50, no. 10, pp. 2401–2405, Oct. 2002.
- [10] A. P. Zhao, "Two special notes on the implementation of the unconditionally stable ADI-FDTD method," *Microw. Opt. Technol. Lett.*, vol. 33, no. 4, pp. 273–277, May 2002.
- [11] H.-L. Chen, B. Chen, Y. Yi, and D.-G. Fang, "Unconditionally stable ADI-BOR-FDTD algorithm for the analysis of rotationally symmetric geometries," *IEEE Microw. Wireless Compon. Lett.*, vol. 17, no. 4, pp. 304–306, Apr. 2007.
- [12] Y.-K. Chung, T. K. Sarkar, H. J. Baek, and M. Salazar-Palma, "An unconditionally stable scheme for the finite-difference time-domain method," *IEEE Trans. Microw. Theory Techn.*, vol. 51, no. 3, pp. 697–704, Mar. 2003.
- [13] H.-L. Chen, B. Chen, Y.-T. Duan, Y. Yi, and D.-G. Fang, "Unconditionally stable Laguerre-based BOR-FDTD scheme for scattering from bodies of revolution," *Microw. Opt. Technol. Lett.*, vol. 49, no. 8, pp. 1897–1900, Aug. 2007.
- [14] I. Ahmed and Z. Chen, "Error reduced ADI-FDTD methods," *IEEE Antennas Wireless Propag. Lett.*, vol. 4, pp. 323–325, 2005.
- [15] Y.-G. Wang, B. Chen, H.-L. Chen, and R. Xiong, "An unconditionally stable one-step leapfrog ADI-BOR-FDTD method," *IEEE Antennas Wireless Propag. Lett.*, vol. 12, pp. 647–650, 2013.
- [16] J. Shibayama, B. Murakami, J. Yamauchi, and H. Nakano, "LOD-BOR-FDTD algorithm for efficient analysis of circularly symmetric structures," *IEEE Microw. Wireless Compon. Lett.*, vol. 19, no. 2, pp. 56–58, Feb. 2009.
- [17] J. Chen and J. Wang, "A novel body-of-revolution finite-difference time-domain method with weakly conditional stability," *IEEE Microw. Wireless Compon. Lett.*, vol. 18, no. 6, pp. 377–379, Jun. 2008.
- [18] Y.-G. Wang, Y. Yi, B. Chen, H.-L. Chen, and K. Luo, "One-step leapfrog weakly conditionally stable finite-difference time-domain method for body of revolution," *IET Microw., Antennas Propag.*, vol. 9, no. 14, pp. 1522–1526, Nov. 2015.
- [19] Y.-G. Wang, Y. Yi, H.-L. Chen, Z. Chen, Y.-T. Duan, and B. Chen, "An efficient laguerre-based BOR-FDTD method using gauss-seidel procedure," *IEEE Trans. Antennas Propag.*, vol. 64, no. 5, pp. 1829–1839, May 2016.

[20] Z. Chen, Y.-T. Duan, Y.-R. Zhang, H.-L. Chen, and Y. Yi, "A new efficient algorithm for 3-D laguerre-based finite-difference time-domain method," *IEEE Trans. Antennas Propag.*, vol. 62, no. 4, pp. 2158–2164, Apr. 2014.

[21] Y.-T. Duan, B. Chen, D.-G. Fang, and B.-H. Zhou, "Efficient implementation for 3-D laguerre-based finite-difference time-domain method," *IEEE Trans. Microw. Theory Techn.*, vol. 59, no. 1, pp. 56–64, Jan. 2011.

[22] J. Chen and J. Wang, "The body-of-revolution hybrid implicit–explicit finite-difference time-domain method with large time step size," *IEEE Trans. Electromagn. Compat.*, vol. 50, no. 2, pp. 369–374, May 2008.

[23] B. D. Welfert, "Analysis of iterated ADI-FDTD schemes for Maxwell curl equations," *J. Comput. Phys.*, vol. 222, no. 1, pp. 9–27, Mar. 2007.

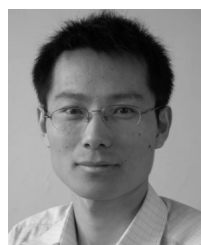
[24] M. Ha, K. Srinivasan, and M. Swaminathan, "Transient chip-package cosimulation of multiscale structures using the Laguerre-FDTD scheme," *IEEE Trans. Adv. Packag.*, vol. 32, no. 4, pp. 816–830, Nov. 2009.

[25] G. Mur, "Absorbing boundary conditions for the finite-difference approximation of the time-domain electromagnetic-field equations," *IEEE Trans. Electromagn. Compat.*, vol. EMC-23, no. 4, pp. 377–382, Nov. 1981.



DA-WEI ZHU was born in Jilin, China, in 1983. He received the B.S. degree in computer science and technology and the M.S. degree in computer system structure from the Changchun University of Science and Technology, Changchun, China, in 2007 and 2011, respectively. He is currently pursuing the Ph.D. degree with the National Key Laboratory on Electromagnetic Environmental Effects and Electro-Optical Engineering, PLA Army Engineering University, Nanjing, China. His

research interest includes computational electromagnetics.



HAI-LIN CHEN was born in Shandong, China, in 1979. He received the B.S. degree from Qingdao University, Shandong, in 2001, and the M.S. and Ph.D. degrees from the Nanjing Engineering Institute, Nanjing, China, in 2004 and 2008, respectively, all in electrical engineering.

He is currently an Associate Professor with the National Key Laboratory on Electromagnetic Environmental Effects and Electro-Optical Engineering, PLA University of Science and Technology, Nanjing. His research interests include computational electromagnetics, lightning protection, and electromagnetic materials.



JIE YANG was born in Jiangsu, China, in 1957. He received the B.S. and M.S. degrees from the Beijing Institute of Technology, Beijing, China, in 1982 and 1987, respectively, and the Ph.D. degree from the Nanjing University of Science and Technology, Nanjing, China, in 1997, all in electrical engineering.

He is currently a Professor with the National Key Laboratory on Electromagnetic Environmental Effects and Electro-Optical Engineering, PLA University of Science and Technology, Nanjing. His research interests include computational electromagnetics and EMP.



YUN YI was born in Hunan, China, in 1978. She received the B.S., M.S., and Ph.D. degrees in electric systems and automation from the Nanjing Engineering Institute, Nanjing, China, in 2000, 2003, and 2006, respectively.

She is currently a Lecturer with the National Key Laboratory on Electromagnetic Environmental Effects and Electro-Optical Engineering, PLA Army Engineering University, Nanjing. Her research interest includes computational electromagnetics.



BIN CHEN (M'98) was born in Jiangsu, China, in 1957. He received the B.S. and M.S. degrees from the Beijing Institute of Technology, Beijing, China, in 1982 and 1987, respectively, and the Ph.D. degree from the Nanjing University of Science and Technology, Nanjing, China, in 1997, all in electrical engineering.

He is currently a Professor with the National Key Laboratory on Electromagnetic Environmental Effects and Electro-Optical Engineering, PLA Army Engineering University, Nanjing. His research interests include computational electromagnetics and EMP.

...